Application of a new kinetic method in the investigation of cleavage reactions of haloaromatic radical anions †

Rasmus J. Enemærke, Torben B. Christensen, Henrik Jensen and Kim Daasbjerg *

Department of Organic Chemistry, University of Aarhus, DK-8000, Aarhus C, Denmark

Received (in Cambridge, UK) 28th March 2001, Accepted 18th June 2001
First published as an Advance Article on the web 20th August 2001

A simple kinetic method based on competition kinetics is presented for the measurement of cleavage rate constants of radical anions over the range of $10^7 - 5 \times 10^9$ s^{-1} in aprotic solvents. The standard potential for the formation of the radical anions may be extracted from the kinetic analysis as well. The method employs electrochemical steady-state or optical detection techniques and is an extension of the redox catalysis approach described previously in the literature. The applicability of the method is illustrated through a systematic study of the cleavage reactions for a number of short-lived haloaromatic radical anions. Interestingly, the radical anion of iodobenzene is found to be an intermediate in the homogeneous reduction of iodobenzene, even though recent investigations have shown that the corresponding heterogeneous reduction at an electrode surface proceeds by a concerted electron transfer-bond cleavage process. The nature of the cleavage reactions is discussed in terms of the activation–driving force plot of the cleavage rate constants *versus* the relevant Gibbs energies. While the exergonic cleavage reactions follow a simple decay mechanism taking place at the halogen site, the endergonic processes are best described as intra-molecular electron transfers from the substituent to the carbon–halogen bond. Nevertheless, the overall intrinsic barrier is found to be relatively small (27–39 kJ mol^{-1}) and it is suggested that the endergonic reactions may proceed by a stepwise mechanism, in which a σ* radical anion is formed as an intermediate prior to the formation of the dissociated products, the aryl radical and the halide. The above conclusions were supported by semi-empirical PM3 calculations of structures and charge distributions in the radical anions.

Introduction

Various techniques may be used in the determination of the cleavage rate constant, k_c, of radical ions. In general, direct detection is to be preferred whenever possible. Techniques such as cyclic voltammetry,[1–5] pulse radiolysis[6–10] and flash photolysis[11] have proven to be convenient and effective tools when the radical ions under study cleave with rate constants smaller than 10^7 s^{-1}. This limit can be pushed further upwards using specialized equipment.[12–15] However, if limitations are imposed on the experimental technique employed due to the very nature of the compound under investigation and/or the presence of a fast cleavage reaction, attention has to be turned to indirect methods. For instance, k_c may be extracted from the characteristics of the linear sweep voltammetric behaviour of the substrate at an electrode.[16] In many cases this approach is not applicable because the mechanism of the electrochemical process as well as the standard potential of the substrate have to be known. A more general approach has consisted of the use of competition kinetics. In particular, the electrochemical redox catalysis method introduced by Savéant *et al*. has been widely employed for determining cleavage rate constants for radical ions in the range $10^6 - 5 \times 10^8$ s^{-1} in aprotic media.[17–22]

In this paper we report on improvements in the redox catalysis method that widen its applicability further and extend the upper limit of accessible rate constants to 5×10^9 s^{-1}. In previous work dealing with radical anions of disulfides some of these features were presented but the full applicability of the approach was not described.[23] The new method has been applied specifically herein in the investigation of short-lived radical anions of various haloaromatic compounds in terms of substituted benzenes, naphthalenes and pyridines in *N*,*N*-dimethylformamide (DMF). Since the standard potential of the haloaromatic compounds may be extracted from the kinetic analysis as well, the driving force of the cleavage processes can be calculated. This allows a detailed and systematic study of the activation–driving force relationship for both exergonic and endergonic cleavage processes and also the possibility of detecting mechanistic shifts. Previous papers have mainly dealt with the influence of specific factors[4,7–9,24–41] and not until recently have systematic investigations of families of compounds appeared.[42–47]

Mechanistic description

In the redox catalysis approach the radical anion of interest, $BX^{\bullet -}$, is formed in a homogeneous electron transfer (ET) process involving the precursor BX and the redox catalyst $A^{\bullet -}$ as shown in eqn. (2) of the following reaction scheme [eqns. (1)–(6)].

$$A + e \rightleftharpoons A^{\bullet -} \quad (1)$$

$$A^{\bullet -} + BX \underset{k_{-ET}}{\overset{k_{ET}}{\rightleftharpoons}} A + BX^{\bullet -} \quad (2)$$

$$BX^{\bullet -} \underset{k_{-c}}{\overset{k_c}{\rightleftharpoons}} B^{\bullet} + X^- \quad (3)$$

$$B^{\bullet} + HS \xrightarrow{k_{abs}} BH + S^{\bullet} \quad (4)$$

$$A^{\bullet -} + B^{\bullet} \xrightarrow{k_5} \text{products} \quad (5)$$

$$A^{\bullet -} + S^{\bullet} \xrightarrow{k_6} \text{products} \quad (6)$$

The species A is usually an aromatic or heteroaromatic compound selected so that its standard potential, E°_A, is positive relative to the standard potential of BX, E°_{BX}. The radical anion $A^{\bullet -}$ is generated by a heterogeneous ET to A at the electrode surface [eqn. (1)]. The cleavage reaction of interest, eqn. (3), can be succeeded by a number of fast follow-up processes, depending on the nature of the radical $B^{\bullet}$. For aryl radicals, hydrogen

† Dedicated to the memory of Professor Lennart Eberson.

 DOI: 10.1039/b102835a

abstraction from the solvent HS as shown in eqn. (4) is a potential reaction path. However, regardless of whether $B^{\bullet}$, a solvent-derived radical $S^{\bullet}$ or a mixture of them is formed in solution their fate is determined by $A^{\bullet -}$ in terms of fast coupling or reduction processes, eqns. (5) and (6).[48,49] Overall, two molecules of $A^{\bullet -}$ are thus used for each molecule of BX.

One interesting feature about the above scheme is the presence of a competition between the first-order cleavage reaction, eqn. (3), and the second-order reverse ET process of eqn. (2). The fact that the competition ratio is dependent on the concentration of A can be exploited in a determination of the rate constant k_c. Savéant and co-workers[17–22] have demonstrated that an electrochemical technique such as linear sweep voltammetry (LSV) can be used in the determination of cleavage rate constants for radical anions in the range $10^6 - 5 \times 10^8$ s^{-1}. In LSV, the upper limit of measurable k_c is set by the maximum concentration of A of about 20 mM which is tolerated without introducing migration of $A^{\bullet -}$ when the concentration of the supporting electrolyte is 0.1 M. Other techniques, however, may not have this limitation, and this would allow the range of accessible k_c values to be extended as a matter of course. With the purpose of investigating this possibility in greater detail three different techniques involving electrochemical steady-state (*i.e.* a rotating disc electrode) or optical detection of $A^{\bullet -}$ (*i.e.* stopped-flow UV or a UV dip probe) have been considered. Common to all of them is the first step in which a certain amount of $A^{\bullet -}$ is generated electrochemically from A. The second step constitutes the actual experiment, where the decay of $A^{\bullet -}$ due to the reaction with BX is recorded as a function of time for varying concentrations of BX and A. In this procedure, there are no restrictions imposed by migration on the maximum value of [A] applicable in the rotating disc electrode technique as long as the amount of $A^{\bullet -}$ generated initially is kept low. Moreover, the somewhat complicating heterogeneous reaction shown in eqn. (1) can be excluded from the analysis of the reaction kinetics.

According to the overall reaction scheme, eqns. (2)–(6), the differential equation for $A^{\bullet -}$ can be expressed as shown in eqn. (7), when the reverse reaction of eqn. (3) is neglected and the steady-state assumption has been imposed on the intermediates $BX^{\bullet -}$, $B^{\bullet}$ and $S^{\bullet}$.

$$d[A^{\bullet -}]/dt = -\beta[A^{\bullet -}], \qquad \text{where} \qquad \beta = \frac{2k_c k_{ET}[BX]}{k_c + k_{-ET}[A]} \quad (7)$$

If the concentrations of BX and A are kept high compared with the initial concentration of $A^{\bullet -}$, the decay of $A^{\bullet -}$ should be confined to a simple pseudo-first-order rate law with an overall rate constant given by β. It is then convenient to introduce the parameter γ defined in eqn. (8).

$$\gamma = \beta/2[BX] = \frac{k_c k_{ET}}{k_c + k_{-ET}[A]} = \frac{k_{ET}}{1 + \frac{k_{-ET}[A]}{k_c}} \quad (8)$$

For the limiting case characterized by the condition $k_c \ll k_{-ET}[A]$, in which kinetic control is by the cleavage process with the ET process acting as a pre-equilibrium, γ approaches $k_c k_{ET}/k_{-ET}[A]$. In the other limit of $k_c \gg k_{-ET}[A]$ with kinetic control by the forward ET reaction, γ approaches k_{ET} and becomes independent of [A].

Two main requirements have to be fulfilled if this method should be used in a determination of k_c. First of all, k_c and k_{-ET} should be of such relative magnitude that a variation of [A] in the range accessible is reflected in an influence on the decay rate of $A^{\bullet -}$. In that instance, measurement of γ at different values of [A] will allow the parameters k_{ET} and the ratio k_c/k_{-ET} to be obtained directly in a non-linear fit of the data to eqn. (8). Alternatively the parameters may be obtained in a linear fit of

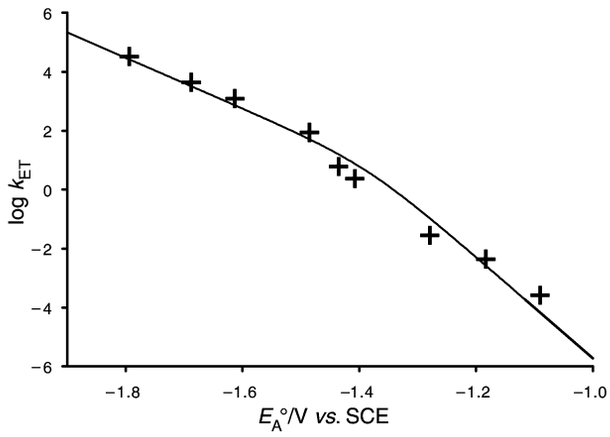

Fig. 1 Plot of log k_{ET} *vs.* E_A° for the reaction of iodobenzene with different aromatic radical anions, $A^{\bullet -}$. The data points pertain to the following sets of (A, E_A°/V *vs.* SCE, log k_{ET}): (9,10-diphenylanthracene, −1.794, 4.52); (fluoranthene, −1.688, 3.64); (perylene, −1.613, 3.09); (1,4-dicyanobenzene, −1.485, 1.94); (1-cyanoisoquinoline, −1.435, 0.79); (1,4-diacetylbenzene, −1.407, 0.38); [(*E*)-azobenzene, −1.279, −1.55]; [(*E*)-4-chloroazobenzene, −1.183, −2.36] and (phenazine, −1.090, −3.59). The solid curve corresponds to the best fit of the data to eqn. (3) in ref. 22 with the following values ensuing when using $\alpha = 0.5$: $k_E^S = 2.8 \times 10^5$ M^{-1} s^{-1} and $E_{BX}^{\circ} = -1.91$ V *vs.* SCE.

$1/\gamma$ against [A]; the intercept at the ordinate provides $1/k_{ET}$ and the slope is given by $k_{-ET}/k_c k_{ET}$ as shown in eqn. (9).

$$1/\gamma = 1/k_{ET} + k_{-ET}[A]/k_c k_{ET} \quad (9)$$

At least from the point of visualization the latter approach is convenient.

Secondly, if the absolute value of the rate constant k_c is to be calculated from the value of k_c/k_{-ET}, then k_{-ET} has to be known. This is the case when the reverse ET is so exergonic that it is controlled by the diffusion together of the two species, and k_{-ET} can be set equal to the diffusion-controlled rate constant k_d. For most systems investigated in DMF the use of $k_d = 10^{10}$ M^{-1} s^{-1} seems appropriate and in accordance with previous assessments.[22,50] For the reaction under investigation it should always be checked that the reverse ET process is placed in the diffusion-controlled region, *i.e.* that a plot of log k_{ET} against E_A° has a slope of $-1/58$ mV^{-1}. In the present study this could be confirmed in each case by comparing the values of k_{ET} and E_A° with those given in ref. 20 or measured herein for at least another mediator. In the case of iodobenzene we carried out an extended study of the relationship between k_{ET} and E_A° since it has been reported recently that the mechanism of the heterogeneous reduction of iodobenzene shifts from a stepwise to a concerted ET–cleavage process as the driving force is lowered.[51] Since the driving force applied in the homogeneous approach is even lower than that used in the heterogeneous approach the radical anion of iodobenzene might not be formed at all under our conditions. Expressed differently, the reverse ET should be precluded and the resulting plot of log k_{ET} *vs.* E_A° is expected to show an activation-controlled region with a slope of *ca.* $-1/116$ mV^{-1} throughout the driving force interval.[22] However, as revealed by the experimental data depicted in Fig. 1 both an activation-controlled and a "counter-diffusion-controlled" region are present indicating that the radical anion of iodobenzene indeed does exist under our conditions. We therefore conclude that all homogeneous reduction processes studied herein follow the stepwise pathway and that k_{-ET} simply can be set equal to k_d in the equations concerned.

The above analysis of the kinetic scheme is based on the assumption that the cleavage occurs completely outside the encounter complex, ($A\ BX^{\bullet -}$), *i.e.* A and $BX^{\bullet -}$ have diffused apart prior to the cleavage process. If the cleavage rate constant should exceed 5×10^8 s^{-1} appreciably, this would not be the

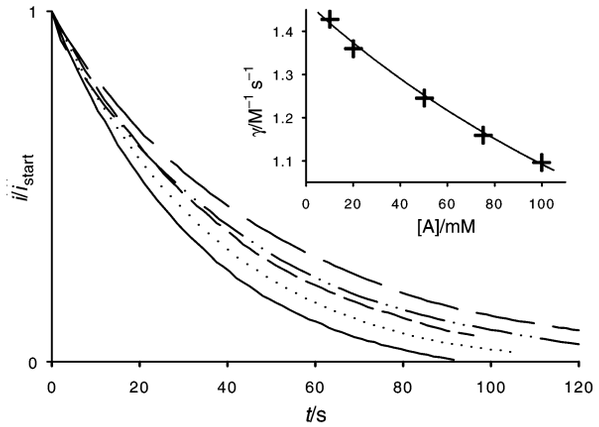

Fig. 2 Decays of the limiting oxidation current of the radical anion of fluoranthene in the reaction with 2-bromopyridine measured by the rotating disc electrode technique for five different concentrations of fluoranthene: [A] = 10 mM, $\gamma = 1.43$ M^{-1} s^{-1} (——); [A] = 20 mM, $\gamma = 1.36$ M^{-1} s^{-1} (· · · · · ·); [A] = 50 mM, $\gamma = 1.25$ M^{-1} s^{-1} (– – –); [A] = 75 mM, $\gamma = 1.16$ M^{-1} s^{-1} (— · · —); [A] = 100 mM, $\gamma = 1.10$ M^{-1} s^{-1} (— —). Inset: Plot of γ *vs.* [A] (+) with the non-linear fit to eqn. (8) shown by the solid curve.

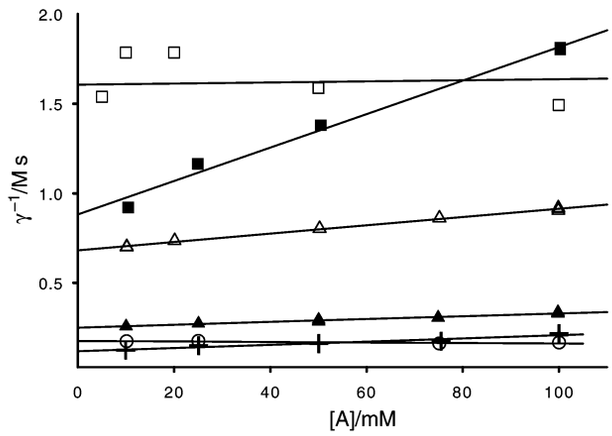

Fig. 3 Plot of γ^{-1} *vs.* [A] for bromobenzene (o), 4-iodobenzonitrile (+), ethyl 4-iodobenzoate (□), 1-bromonaphthalene (■), 2-bromopyridine (△) and 3-bromopyridine (▲). Linear regression fits to eqn. (9) are included as solid lines.

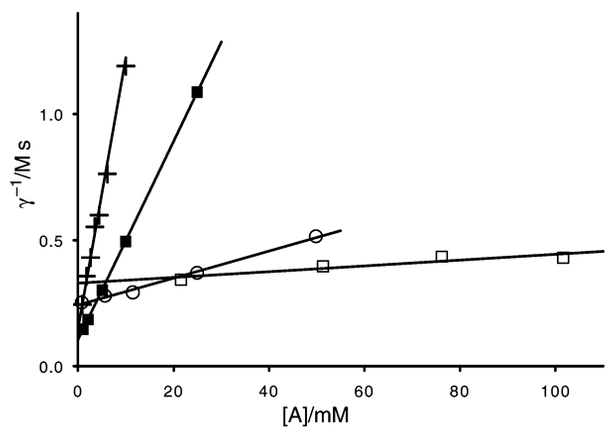

Fig. 4 Plot of γ^{-1} *vs.* [A] for 4-chlorobenzonitrile (o), ethyl 4-chlorobenzoate (+), 4-iodoacetophenone (□) and 1-chloronaphthalene (■). Linear regression fits to eqn. (9) are included as solid lines.

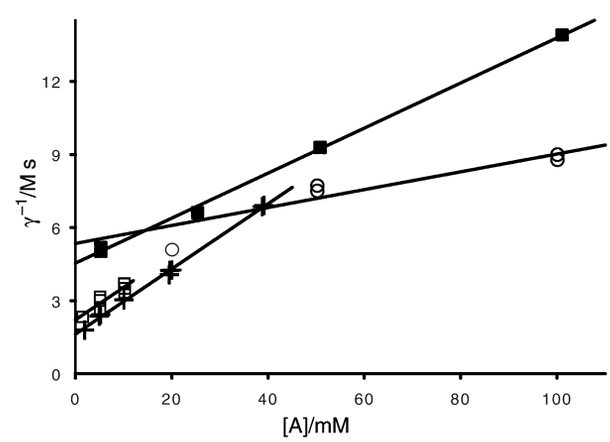

Fig. 5 Plot of γ^{-1} *vs.* [A] for 2-bromoacetophenone (o), 4-iodobenzophenone (+), 3-iodoacetophenone (□) and 2-bromonaphthalene (■). Linear regression fits to eqn. (9) are included as solid lines.

case and large values of [A] would be required for accomplishing a competition situation. As a consequence, the original Smoluchowski calculation derived for diffusion-controlled reactions in dilute solutions cannot be applied. In principle, the theory of non-equilibrium statistical thermodynamics might then be considered[52,53] but this would clearly remove the simplicity and generality of the presented method. Therefore, we decided to base our investigation on the simple kinetic scheme, keeping in mind then that the upper limit on attainable k_c determined from eqn. (7) is set by $k_c/k_d \approx 0.5$ M, *i.e.* $k_c \approx 5 \times 10^9$ s^{-1}. For faster cleavage reactions rough estimations of k_c of up to 2×10^{10} s^{-1} can still be provided.

With the knowledge of k_{ET} and E°_A, the standard potential of BX, E°_{BX}, is easily extracted from the relationship given in eqn. (10).

$$k_{ET} = k_d \exp[F(E^\circ_{BX} - E^\circ_A)/RT] \qquad (10)$$

Strictly speaking, this expression can be used only if the cleavage process occurs completely outside the encounter complex (A $BX^{\bullet -}$), but detailed analyses have shown that the error on E°_{BX} constitutes less than 100 mV when 5×10^8 $s^{-1} < k_c < 6 \times 10^{12}$ s^{-1}.[22,54]

Results and discussion

Methodology

According to eqn. (7) the decay of $A^{\bullet -}$ should follow a pseudo-first-order rate law if sufficiently large concentrations of A and BX are used. This prediction is borne out by experiments. In Fig. 2 the results obtained by means of the rotating disc electrode technique are shown for the reaction between the radical anion of fluoranthene and 2-bromopyridine. The limiting oxidation current of $A^{\bullet -}$ is measured against time for different values of [A] and as expected the rate of decay becomes slower as [A] is increased. From the best exponential fits the parameters β and γ are determined. The inset shows a plot of γ *vs.* [A], allowing the extraction of k_{ET} and k_c/k_d from a non-linear fit to eqn. (8). In Figs. 3–6 all data are collected as plots of γ^{-1} *vs.* [A] together with the best linear fits to eqn. (9), which gives access to the rate constants of interest from the intercept, $1/k_{ET}$, and the slope, $k_d/k_c k_{ET}$. The results obtained from the regression analyses are gathered in Table 1 together with literature values.[21,22,55–57]

One point neglected so far is the possible influence by the reverse reaction of the cleavage process, eqn. (3), as observed in the study concerning the radical anion of diphenyl disulfide.[23] From a kinetic point of view, deviation from the simple pseudo-first-order rate law should be observable if this reaction is of substantial importance due to the increase in the concentration of X^- as the overall reaction proceeds. For none of the substrates investigated could this situation ever be observed. Even the addition of 0.1 M tetrabutylammonium iodide to the reaction between the radical anion of 1,4-dicyanobenzene and 2-iodopyridine or the addition of 0.1 M tetrabutylammonium

Table 1 Electron transfer rate constants, k_{ET}, and cleavage rate constants, k_c, determined for different combinations of mediators A and substrates BX at 20 °C in DMF. The uncertainty in k_{ET} is estimated to be 20%

BX	A	E°_{A} [a]	k_{ET} [b]	k_c/k_d [c]	k_c [d,e] (This study)	k_c [d] (Lit.)
Chlorobenzene	*m*-Toluonitrile	−2.264	31	>2	$>2 \times 10^{10}$ [f]	$\leq 1.5 \times 10^{11}$ [g]
Bromobenzene	Anthracene	−1.890	5.7	>2	$>2 \times 10^{10}$ [f]	$\leq 1.5 \times 10^{11}$ [g]
Iodobenzene	(*E*)-Azobenzene	−1.279	0.028	>2	$>2 \times 10^{10}$ [f]	
4-Chlorobenzonitrile	1,4-Dicyanobenzene	−1.485	4.1	4.5×10^{-2}	$4.5(\pm 0.9) \times 10^{8}$ [i]	5.0×10^{8} [j] 9.3×10^{8} [k]
4-Bromobenzonitrile	1,4-Dicyanobenzene	−1.485	290	6.0×10^{-2}	$6.0(\pm 1.2) \times 10^{8}$ [i]	1.0×10^{10} [l]
	(*E*)-2,4-Dimethoxyazobenzene	−1.416	3.9	4.7×10^{-2}	$4.7(\pm 0.9) \times 10^{8}$ [f]	2.0×10^{9} [k]
4-Iodobenzonitrile	(*E*)-Azobenzene	−1.279	8.4	1.3×10^{-1}	$1.3(\pm 0.4) \times 10^{9}$ [f]	5.0×10^{10} [l] 2.5×10^{10} [k]
Ethyl 4-chlorobenzoate	1,4-Dicyanobenzene	−1.485	7.0	1.3×10^{-3}	$1.3(\pm 0.3) \times 10^{7}$ [f]	
Ethyl 4-bromobenzoate	1,4-Dicyanobenzene	−1.485	44	2.0×10^{-1}	$2.0(\pm 0.6) \times 10^{9}$ [i]	
Ethyl 4-iodobenzoate	(*E*)-Azobenzene	−1.279	0.62	>2	$>2 \times 10^{10}$ [f]	
2-Bromoacetophenone	Fluoren-9-one	−1.217	0.19	1.5×10^{-1}	$1.5(\pm 0.5) \times 10^{9}$ [f]	5.1×10^{9} [m]
3-Iodoacetophenone	Benzanthrone	−1.164	0.45	1.7×10^{-2}	$1.7(\pm 0.3) \times 10^{8}$ [f]	1.9×10^{8} [m]
4-Iodoacetophenone	Fluoren-9-one	−1.217	3.0	2.8×10^{-1}	$2.8(\pm 0.8) \times 10^{9}$ [f]	3.5×10^{9} [m]
4-Iodobenzophenone	(*E*)-4-Methoxycarbonylazobenzene	−1.015	0.62	1.2×10^{-2}	$1.2(\pm 0.2) \times 10^{8}$ [f]	
1-Chloronaphthalene	Fluoranthene	−1.688	9.7	2.6×10^{-3}	$2.6(\pm 0.5) \times 10^{7}$ [i]	5.0×10^{7} [n]
1-Bromonaphthalene	Quinoxaline	−1.589	1.1	1.1×10^{-1}	$1.1(\pm 0.3) \times 10^{9}$ [f]	3.0×10^{8} [n]
				1.1×10^{-1}	$1.1(\pm 0.2) \times 10^{9}$ [h]	2.0×10^{8} [o]
1-Iodonaphthalene	1,4-Dicyanobenzene	−1.485	370	1.5×10^{-1}	$1.5(\pm 0.4) \times 10^{9}$ [i]	6×10^{8} [o] 4×10^{10} [l]
2-Bromonaphthalene	Quinoxaline	−1.589	0.22	4.7×10^{-2}	$4.7(\pm 0.8) \times 10^{8}$ [f]	
				5.1×10^{-2}	$5.1(\pm 1.0) \times 10^{8}$ [h]	
2-Chloropyridine	2-Naphthonitrile	−1.880	38	4.2×10^{-1}	$4.2(\pm 1.3) \times 10^{9}$ [i]	$\leq 2.3 \times 10^{9}$ [g]
2-Bromopyridine	Fluoranthene	−1.688	1.5	2.9×10^{-1}	$2.9(\pm 0.9) \times 10^{9}$ [f]	$\leq 1.5 \times 10^{10}$ [g]
2-Iodopyridine	1,4-Dicyanobenzene	−1.485	330	4.6×10^{-1}	$4.6(\pm 1.4) \times 10^{9}$ [i]	
3-Chloropyridine	2-Naphthonitrile	−1.880	67	3.6×10^{-1}	$3.6(\pm 1.1) \times 10^{9}$ [i]	$\leq 6 \times 10^{8}$ [g]
3-Bromopyridine	Fluoranthene	−1.688	4.0	3.2×10^{-1}	$3.2(\pm 1.0) \times 10^{9}$ [f]	$\leq 4.8 \times 10^{10}$ [g]

[a] In V *vs.* SCE. [b] In $M^{-1}\ s^{-1}$. [c] In M. [d] In s^{-1}. [e] Calculated using $k_d = 10^{10}\ M^{-1}\ s^{-1}$. [f] Determined by the rotating disc electrode technique. [g] From ref. 22, in DMF. [h] Determined by the UV dip probe technique. [i] Determined by the stopped-flow UV technique. [j] From ref. 21, in acetonitrile. [k] From ref. 56, in ammonia at −38 °C. [l] From ref. 55, in acetonitrile. [m] From ref. 57, in acetonitrile. [n] From ref. 21, in dimethyl sulfoxide. [o] From ref. 55, in dimethyl sulfoxide.

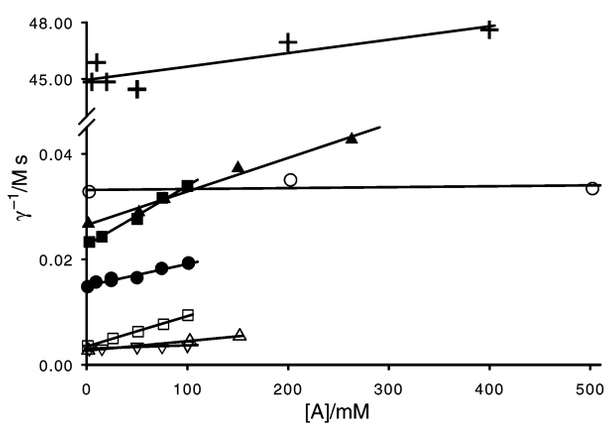

Fig. 6 Plot of γ^{-1} *vs.* [A] for chlorobenzene (o), iodobenzene (+), 4-bromobenzonitrile (□), ethyl 4-bromobenzoate (■), 1-iodonaphthalene (△), 2-chloropyridine (▲), 2-iodopyridine (▽) and 3-chloropyridine (●). Linear regression fits to eqn. (9) are included as solid lines.

chloride to the reaction between the radical anion of 1,4-dicyanobenzene and 4-chlorobenzonitrile had no influence on the reaction kinetics of $A^{\bullet -}$. In conclusion, these results show that the reverse reaction of eqn. (3) is not able to compete with the fast follow-up processes shown in eqns. (4)–(6). On the assumption that reactions (5) and (6) are under diffusion-control ($k_d = 10^{10}\ M^{-1}\ s^{-1}$) and that $k_{-c}[X^-]/k_d[A^{\bullet -}]$ should be at least 0.1 in order to detect the reverse reaction, it follows that the highest value of k_{-c} possible is $10^6\ M^{-1}\ s^{-1}$ when $[X^-]/[A^{\bullet -}] = 1000$.

The cleavage rate constants determined by the new kinetic method range from $1.3 \times 10^7\ s^{-1}$ for the radical anion of ethyl 4-chlorobenzoate to a value larger than $2 \times 10^{10}\ s^{-1}$ for the radical anions of ethyl 4-iodobenzoate and the halobenzenes. It is gratifying to note the agreement observed between the results obtained by means of two different techniques such as the rotating disc electrode and UV dip probe in the investigation of the radical anions of 1- and 2-bromonaphthalene. Moreover, the determination of k_c is not influenced by the choice of mediator as illustrated by the use of the two different compounds, 1,4-dicyanobenzene and (*E*)-2,4-dimethoxyazobenzene, in the investigation of 4-bromobenzonitrile radical anion. It is difficult to carry out a comparison of the present results with the literature values listed in column 7 of Table 1 due to differences in medium and temperature. In general, there seems to be agreement but some inconsistencies are also present when, for instance, the almost equal rate constants obtained for 4-chlorobenzonitrile in DMF and acetonitrile are related to the deviation of a factor of twenty observed in the corresponding case of 4-bromobenzonitrile. At present we have no explanations for this discrepancy.

The kinetic method presented in this paper has advantages compared to the "normal" redox catalysis approach using LSV. The first one is related to the fact that the LSV technique can be applied to systems in which γ is in the range $10 - 10^5\ M^{-1}\ s^{-1}$, whereas the characteristic time window of the techniques used herein corresponds to γ in the range $10^{-3} - 500\ M^{-1}\ s^{-1}$. The lower limit may vary somewhat from one species to another and from one experiment to another since it is settled by the stability of $A^{\bullet -}$ prior to the addition of BX. In any case, having such a low limit for γ enhances the possibility of accomplishing a situation where the reverse ET is under diffusion control even if it is considerably slowed down by a large intrinsic barrier.[23]

The second point is that the current obtained in the LSV method is dependent on which products are formed in eqns. (5) and (6), *i.e.* the amount of A regenerated in the competing coupling and reduction reactions of $A^{\bullet -}$ with either $B^{\bullet}$ or $S^{\bullet}$.[48] These reactions have to be taken specifically into account in the simulation procedure. In the new kinetic method, on the other hand, they have no influence on the reaction kinetics pertaining to $A^{\bullet -}$ and many mechanistic schemes will be confined to the rate law given by eqns. (7) and (8).

The third advantage is that [A] in the order of 10^{-3} − 0.5 M can be employed in the kinetic method as long as limitations due to impurities or insolubility do not arise. The determination of cleavage rate constants in the range $10^7 - 5 \times 10^9$ s^{-1} should therefore be in reach, which is an extension of the upper limit by a factor of ten compared to the LSV method. For even faster cleavage reactions with k_c of up to 2×10^{10} s^{-1} a rough estimation can still be provided even if the interpretation of the kinetic data is subtle because of the large concentrations of A required. The lower limit of 10^7 s^{-1} can be diminished if the restriction imposed on [A] by the pseudo-first-order condition, [A] > 10[$A^{\bullet -}$], is abandoned. However, an exact knowledge of the reaction stoichiometry would then be required as the variation in [A] should be taken specifically into account in the data treatment.

Haloaromatic radical anions

In Table 2 we have collected all relevant cleavage rate constants, k_c, and standard potentials, E°_{BX}, for haloaromatic radical anions investigated herein for the fast reactions ($k_c > 10^7$ s^{-1}) or available in literature for mainly the slower processes.[3,5,24,31,57–61] For most radical anions k_c increases in the halogen order Cl < Br < I in agreement with the findings of other studies.[14,28,58] However, this trend is not equivocally pronounced for all systems. Whereas the variation in k_c going from X = Cl to X = I is large for the radical anions of 4-nitro-, 3-acetyl- and 4-acetylhalobenzenes, constituting as much as a factor of 10^8, k_c is found to be essentially the same in each case of the radical anions of the 1- and 2-halonaphthalenes, the 4-halobenzonitriles and in particular the 2- and 3-halopyridines. As to the three ethyl 4-halobenzoates, a sort of intermediate behaviour is observed. Thus, it seems to be a general trend that simple aromatic systems cleave with a rate that is relatively independent of the nature and position of X but as the aromatic system becomes further extended or substituted with electron attracting groups the effect of X on k_c comes through. In some respects, this behaviour may be compared to recent results obtained for the intra-molecular non-dissociative charge separation in donor–acceptor systems separated by molecular bridges.[62] Depending on the energy levels of the three units, the bridges are in some cases able to assist the electron transfer processes. Within our systems the donor, acceptor and bridge correspond to the substituent, the halogen and the phenyl ring.

The values of E°_{BX} calculated from eqn. (10) are listed in column 3 of Table 2. For chlorobenzene, bromobenzene, 2-chloro-, 3-chloro-, 2-bromo- and 3-bromopyridine they are consistent within 100 mV with a previous and more thorough determination using several pairs of k_{ET} and E°_A.[20,22] With these values in hand it is now possible to calculate the Gibbs energy of the cleavage process, $\Delta G^\circ_{BX^{\bullet -}}$. This parameter can easily be estimated on the basis of a thermochemical cycle incorporating the bond dissociation Gibbs energy of the carbon–halogen bond in BX, $BDFE_{BX}$, and the standard potentials, E°_{BX} and $E^\circ_{X^\bullet}$, as shown in eqn. (11).[63]

$$\Delta G^\circ_{BX^{\bullet -}} = BDFE_{BX} + F(E^\circ_{BX} - E^\circ_{X^\bullet}) \qquad (11)$$

The reverse step of the cleavage process, *i.e.* coupling between a radical and an anion, is of much interest since it presents an essential step of the $S_{RN}1$ process.[64–66] The values of $E^\circ_{X^\bullet}$ in DMF are obtained by combining the corresponding average values tabulated for water[67] and the relevant transfer energies of the halides between water and DMF.[68] The transfer energies of the halogen atoms are assumed to be negligible. The values of $BDFE_{BX}$ can be calculated from bond dissociation energies of BX, BDE_{BX},[63] obtained for the whole series of compounds by means of PM3 calculations. The BDE_{BX} and $\Delta G^\circ_{BX^{\bullet -}}$ values are included in Table 2. The uncertainty on $\Delta G^\circ_{BX^{\bullet -}}$ is in the order of ±15 kJ mol^{-1} which mainly is due to the high uncertainty associated with the estimation of $E^\circ_{X^\bullet}$. The fact that the reverse reaction in the case of 4-chlorobenzonitrile is not kinetically detectable (*i.e.* $k_c \leq 10^6$ M^{-1} s^{-1}), even though $\Delta G^\circ_{BX^{\bullet -}} = 0$ kJ mol^{-1}, might suggest that the calculated values of $\Delta G^\circ_{BX^{\bullet -}}$ are slightly overestimated. Still, the consistency in the relative values is high.

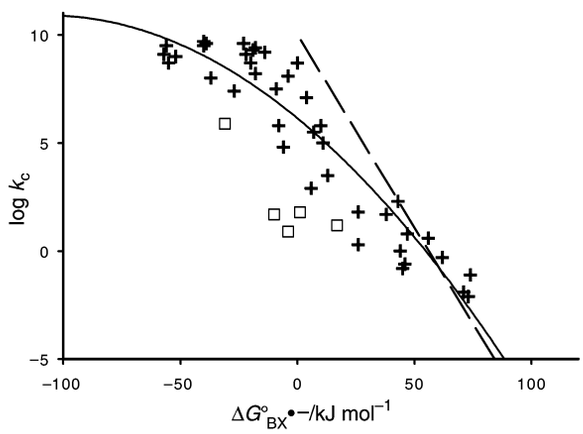

Fig. 7 Plot of log k_c *vs.* $\Delta G^\circ_{BX^{\bullet -}}$ for a number of haloaromatic radical anions. The parabolic curve is obtained as the best fit of the experimental data to eqn. (16), excluding the data points pertaining to the haloanthracenes (□). The dashed straight line with a slope of −0.178 mol kJ^{-1} corresponds to the diffusion-controlled zone, where $k_{-c} = k_d = 10^{10}$ M^{-1} s^{-1}.

The development in the absolute values of $\Delta G^\circ_{BX^{\bullet -}}$, for the three halogen compounds in a given series of $BX^{\bullet -}$ is a result of the opposing effects of $BDFE_{BX}$, E°_{BX} and $E^\circ_{X^\bullet}$. The bond dissociation Gibbs energy, $BDFE_{BX}$, favours the cleavage process in the order I > Br > Cl whereas the contribution from both sets of potentials in most cases works in the opposite direction. An important point in this context is that E°_{BX}, contrary to $BDFE_{BX}$ and obviously $E^\circ_{X^\bullet}$ is dependent on the nature of the substituent positioned on the aromatic system. The largest difference in E°_{BX} is observed for the simplest substrates, *i.e.* the halobenzenes and halopyridines, while the effect becomes smaller and vanishes as electron attracting substituents or extended conjugation is present in the aromatic systems. Interestingly, the reason for this behaviour is almost solely due to the enormous variation in E°_{BX} for the chloro compounds, which ranges from −2.76 to −1.05 V *vs.* SCE going from chlorobenzene to 4-chloronitrobenzene whereas E°_{BX} essentially is constant and equal to -1.82 ± 0.10 V *vs.* SCE for all iodo compounds investigated, the exceptions being the two iodonitrobenzenes with $E^\circ_{BX} \approx -1$ V *vs.* SCE. Note also that many of the cleavage reactions are endergonic (*i.e.* $\Delta G^\circ_{BX^{\bullet -}} > 0$) and accordingly the reverse reaction should be feasible.

In Fig. 7 the cleavage rate constants are correlated with $\Delta G^\circ_{BX^{\bullet -}}$ in an activation–driving force plot, where the limiting k_c values obtained for the halobenzenes, ethyl 4-iodobenzoate and 4-chloronitrobenzene have been omitted. The plot is widely scattered which indeed is expected when there is a variation in the structural and electronic features of the compounds concerned. Still, the decrease in k_c as a function of $\Delta G^\circ_{BX^{\bullet -}}$ throughout the driving force interval is pronounced. The largest deviations are seen for the relatively slow cleavage processes of the radical anions of the haloanthracenes, which presumably is due to the extensive delocalization of the unpaired electron in these cases. On the other hand, there is no distinct behaviour observed for each of the halide families, so evidently the same activation–driving force relationship applies to the iodides, bromides and chlorides. It is also somewhat surprising that the *meta*-compounds are so "well-behaved" since it is known for other types of systems such as the radical anions of nitrobenzyl halides that the cleavage rate constants are highly dependent on the position of the nitro group relative to the CH_2X group.[7]

Table 2 Cleavage rate constants, k_c, standard potentials, E°_{BX}, bond dissociation energies of the carbon–halogen bond in BX, BDE_{BX}, and Gibbs energies of the cleavage process, $\Delta G^\circ_{BX^{\cdot-}}$, in DMF

BX	log k_c [a]	E°_{BX} [b]	BDE_{BX} [c]	$\Delta G^\circ_{BX^{\cdot-}}$ [d]	$\Delta G^{\ddagger}_o$ [e]	
Chlorobenzene	>10.3	−2.76	400	−70	<27	<43
Bromobenzene	>10.3	−2.43	337	−65	<26	<41
Iodobenzene	>10.3	−1.91	274	−32	<15	<29
4-Chlorobenzonitrile	8.7	−2.03	399	0	13	24
4-Bromobenzonitrile	8.7	−1.94	335	−20	21	33
4-Iodobenzonitrile	9.1	−1.81	274	−22	20	32
Ethyl 4-chlorobenzoate	7.1	−2.02	403	4	19	31
Ethyl 4-bromobenzoate	9.3	−1.97	339	−19	17	29
Ethyl 4-iodobenzoate	>10.3	−1.87	273	−29	<14	<28
2-Chlorobenzaldehyde	2.3 [f]	−1.56 [f]	397	43	22	35
2-Chloroacetophenone	5.5 [g]	−1.90 [h]	394	7	27	38
2-Bromoacetophenone	9.2	−1.84	331	−14	16	28
3-Chloroacetophenone	0.3 [i]	−1.76 [i]	399	26	46	58
3-Bromoacetophenone	4.8 [j]	−1.81 [j]	337	−6	37	49
3-Iodoacetophenone	8.2	−1.77	274	−18	23	35
4-Chloroacetophenone	3.5 [k]	−1.90 [l]	400	13	35	47
4-Bromoacetophenone	7.5 [l]	−1.84 [l]	336	−9	24	35
4-Iodoacetophenone	9.4	−1.77	274	−18	16	29
2-Chlorobenzophenone	1.8 [g]	−1.70 [f]	394	26	37	49
3-Bromobenzophenone	2.9 [g]	−1.63 [h]	331	6	42	54
4-Chlorobenzophenone	1.7 [l]	−1.64 [l]	400	38	29	42
4-Bromobenzophenone	5.0 [l]	−1.63 [l]	336	11	27	39
4-Iodobenzophenone	8.1	−1.61	273	−4	18	29
4,4′-Dichlorobenzophenone	0.8 [m]	−1.55 [f]	400	47	28	42
3-Iodonitrobenzene	−0.3 [n]	−0.94 [o]	274	62	20	37
4-Chloronitrobenzene	<−4 [p]	−1.05 [l]	401	96	[q]	[q]
4-Bromonitrobenzene	−2.1 [n]	−0.98 [l]	335	73	21	40
4-Iodonitrobenzene	0.6 [n]	−1.00 [o]	274	56	20	36
3-Bromo-4-methylnitrobenzene	−1.1 [l]	−0.98 [l]	336	74	[q]	32
4-Bromo-3-methylnitrobenzene	−1.9 [l]	−1.00 [l]	335	71	23	41
4-Bromo-3,5-dimethylnitrobenzene	0.0 [l]	−1.27 [l]	334	44	36	49
1-Bromofluorenone	−0.8 [l]	−1.20 [l]	329	45	40	52
3-Bromofluorenone	−0.6 [l]	−1.19 [l]	329	46	38	51
1-Chloronaphthalene	7.4	−2.21	390	−27	32	44
1-Bromonaphthalene	9.0	−2.17	325	−52	31	45
1-Iodonaphthalene	9.2	−1.92	250	−57	32	45
2-Chloronaphthalene	8.0 [l]	−2.30 [l]	389	−37	32	44
2-Bromonaphthalene	8.7	−2.21	326	−55	34	48
1-Chloroanthracene	0.9 [l]	−1.73 [l]	367	−4	58	70
2-Chloroanthracene	1.7 [l]	−1.80 [l]	367	−10	57	68
9-Chloroanthracene	1.8 [i]	−1.66 [i]	365	1	50	62
9-Bromoanthracene	5.9 [j]	−1.68 [j]	299	−31	42	54
9,10-Dichloroanthracene	1.2 [r]	−1.47 [r]	362	17	46	58
2-Chloropyridine	9.6	−2.37	393	−39	23	36
2-Bromopyridine	9.5	−2.26	330	−56	29	43
2-Iodopyridine	9.7	−1.92	267	−40	22	36
3-Chloropyridine	9.6	−2.36	408	−23	17	30
3-Bromopyridine	9.5	−2.23	343	−40	24	37
2-Chloroquinoline	5.8 [l]	−1.92 [l]	381	−8	32	44
4-Chloroquinoline	5.8 [l]	−1.89 [l]	396	10	23	35

[a] This work unless otherwise indicated. [b] In V *vs.* SCE, this work unless otherwise indicated. [c] In kJ mol^{-1}, obtained by means of PM3 calculations. [d] In kJ mol^{-1}, calculated from eqn. (11), where $BDFE_{BX} = BDE_{BX} - T(S^\circ_{X^\cdot} + \Delta S^\circ_{sol,X^\cdot})$. The following standard potentials[67,68] (see text) and entropies[63] were used: $E^\circ_{Cl^\cdot} = 1.8$, $E^\circ_{Br^\cdot} = 1.4$ and $E^\circ_{I^\cdot} = 0.9$ V *vs.* SCE, $S^\circ_{Cl^\cdot} = 165.2$, $S^\circ_{Br^\cdot} = 175.0$, $S^\circ_{I^\cdot} = 180.8$ and $\Delta S^\circ_{sol,X^\cdot} = -63$ J mol^{-1} K^{-1}. [e] In kJ mol^{-1}, calculated from eqn. (16) for $Z = 8 \times 10^{10}$ and 10^{13} s^{-1}, respectively. [f] Measured by cyclic voltammetry at 20 °C. [g] From ref. 57, measured in acetonitrile at room temperature. [h] Assumed to be the same as for the *para*-compound. [i] From ref. 31, measured at 20 °C. [j] From ref. 58, measured at 25 °C. [k] From ref. 5, measured in acetonitrile at room temperature. [l] From ref. 24, measured at 25 °C. [m] From ref. 3, measured at 22 °C. [n] From ref. 59, obtained at 20 °C by extrapolation of measurements carried out at different temperatures. [o] From ref. 60, measured at 23 °C. [p] The decay of the electrogenerated radical anions was measured potentiostatically at a rotating disc electrode at 20 °C. [q] Eqn. (16) provides no solutions. [r] From ref. 61, measured at 25 °C.

Before analysing the plot in greater detail it should be considered whether the endergonic cleavage reactions might be kinetically controlled by out-of-cage diffusion of the dissociated products as seen in studies on radical anions of α-aryloxyacetophenones[46] and radical cations of *tert*-butylated NADH analogues.[69] A diffusion-controlled zone with a slope of −0.178 mol kJ^{-1} as shown by the dashed straight line in Fig. 7 should appear when the coupling reaction of B$^\bullet$ and X$^-$ becomes diffusion-controlled, *i.e.* $k_{-c} = k_d = 10^{10}$ M^{-1} s^{-1}.‡ The rate data for the nitro-substituted haloaromatic compounds are positioned close to this line and indeed it has been reported in the literature that the cleavage process of the radical anion of 4-iodonitrobenzene is reversible although the reverse reaction is

‡ The complete kinetic scheme for the cleavage process incorporates diffusion steps as depicted below.[69]

$$(BX^{\cdot-}) \underset{k^-_c}{\overset{k^+_c}{\rightleftharpoons}} (B^\cdot X^-) \underset{k_d}{\overset{k_{-d}}{\rightleftharpoons}} B^\cdot + X^-$$

The expressions for the two overall rate constants k_c and k_{-c} are given by:

$$k_c = \frac{k_{-d}k^+_c}{k_{-d} + k^-_c} \quad \text{and} \quad k_{-c} = \frac{k_d k^-_c}{k_{-d} + k^-_c}$$

For the diffusion-controlled zone: $k_{-c} \gg k_{-d}$, *i.e.* $k_c = k_{-d}k^+_c/k^-_c = k_{-d}\exp(-\Delta G^\circ_{BX^{\cdot-}}/RT)$, where $k_{-d} = 10^{10}$ s^{-1}.

not completely diffusion-controlled.[59] It should also be recalled that our kinetic analysis allowed the maximum value of k_{-e} to be settled at 10^6 M^{-1} s^{-1} for the radical anions listed in Table 1. On this basis we conclude that the data depicted in Fig. 7 mainly pertain to the activation-controlled zone.

With the purpose of extracting information about the magnitude of the intrinsic barriers for the cleavage processes we employ the model developed by Savéant, in which the potential energy of the radical anion can be approximated by a Morse curve. The following quadratic activation–driving force relationship ensues, eqn. (12), where $\Delta G^{\ddagger}$ is the activation energy and $\Delta G^{\ddagger}_{o}$ the intrinsic barrier:[70]

$$\Delta G^{\ddagger} = \Delta G^{\ddagger}_{o}(1 + \Delta G^{o}_{BX^{\bullet-}}/4\Delta G^{\ddagger}_{o})^2 \quad (12)$$

The intrinsic barrier is composed of two components as shown in eqn. (13), where $4\Delta G^{\ddagger}_{o,i}$ is the inner reorganization energy and λ_o the solvent reorganization energy.

$$4\Delta G^{\ddagger}_{o^-} = 4\Delta G^{\ddagger}_{o,i} + \lambda_o \quad (13)$$

When the unpaired electron is mainly located on B in $BX^{\bullet-}$, $4\Delta G^{\ddagger}_{o,i}$ is determined as shown in eqn. (14), where $E^{o}_{B^{\bullet}/(B^{\bullet})^{-}}$ corresponds to the oxidation potential of an excited state of B^- and ΔS is the entropy change.[70]

$$4\Delta G^{\ddagger}_{o,i} = BDE_{BX} + F(E^{o}_{BX} - E^{o}_{B^{\bullet}/(B^{\bullet})^{-}}) + T\Delta S \quad (14)$$

If the electron is mainly located on X, $4\Delta G^{\ddagger}_{o,i}$ is given by eqn. (15), where $E^{o}_{X^{\bullet}/(X^{\bullet})^{-}}$ corresponds to the oxidation potential of an excited state of X^-.[70]

$$4\Delta G^{\ddagger}_{o,i} = BDE_{BX} + F(E^{o}_{BX} - E^{o}_{X^{\bullet}/(X^{\bullet})^{-}}) + T\Delta S \quad (15)$$

The quadratic relationship given between $\log k_e$ and $\Delta G^{o}_{BX^{\bullet-}}$ in eqn. (16) is easily derived by combining eqn. (12) with the

$$\log k_e = \log Z - \Delta G^{\ddagger}/RT\ln 10 = \log Z - \Delta G^{\ddagger}_{o}/RT\ln 10 - \Delta G^{0}_{BX^{\bullet-}}/2RT\ln 10 - \Delta G^{o}_{BX^{\bullet-}}{}^2/16RT\ln 10\,\Delta G^{\ddagger}_{o} \quad (16)$$

Eyring equation, where Z denotes the pre-exponential parameter.

The best fit of the experimental data to eqn. (16) using $Z = 10^{13}$ s^{-1} leads to $\Delta G^{\ddagger}_{o} = 39 \pm 20$ kJ mol^{-1}, excluding the strongly deviating data points pertaining to the radical anions of the haloanthracenes. Also, it is assumed that all rate constants are activation-controlled. If Z is allowed to vary in the regression analysis, the better (but not particularly good) fit shown in Fig. 7 is obtained with $Z = 8 \times 10^{10}$ s^{-1} and $\Delta G^{\ddagger}_{o} = 27 \pm 9$ kJ mol^{-1} ensuing. Since Z is not expected to exceed 10^{13} s^{-1} we conclude that the overall $\Delta G^{\ddagger}_{o}$ for the cleavage processes studied is in the range 27–39 kJ mol^{-1}. Obviously, the variation in the individual $\Delta G^{\ddagger}_{o}$ values is much higher due to the large scattering of the points in Fig. 7. In Table 2 we have listed $\Delta G^{\ddagger}_{o}$ for all compounds, calculated from eqn. (16) using $Z = 8 \times 10^{10}$ and 10^{13} s^{-1}, respectively. For the former case $\Delta G^{\ddagger}_{o}$ varies from 13 kJ mol^{-1} for 4-chlorobenzonitrile to 58 kJ mol^{-1} for 1-chloroanthracene. The finding of large values of $\Delta G^{\ddagger}_{o}$ for the haloanthracenes is expected in the sense that the pertinent rate constants in these cases were the most deviating ones in Fig. 7. For most compounds but the series of halobenzonitriles, halonaphthalenes and halopyridines, $\Delta G^{\ddagger}_{o}$ increases in the halogen order I < Br < Cl; this is in accordance with the presence of BDE_{BX} in the expression given in eqn. (14) for $\Delta G^{\ddagger}_{o,i}$. The data also show that there is no clear-cut dependence of $\Delta G^{\ddagger}_{o}$ on $\Delta G^{o}_{BX^{\bullet-}}$.

The overall values of $\Delta G^{\ddagger}_{o} = 27$–$39$ kJ mol^{-1} for the haloaromatic radical anions are comparable to the intrinsic barrier of 34 kJ mol^{-1} obtained for the cleavage reaction of the radical anions of α-aryloxyacetophenones using $Z = 10^{13}$ s^{-1}.[46] In a study of the C–C bond cleavage of a number of bibenzylic radical anions and cations the intrinsic barrier was reported to be even lower[42] but the interpretation of the experimental results was subtle in this case due to kinetic control by the out-of-cage diffusion for some of the cleavage reactions.[69] For a series of α-substituted acetophenone radical anions, $\Delta G^{\ddagger}_{o}$ was estimated to be in the order of 70 kJ mol^{-1}.[43,44]

The intrinsic barriers obtained herein are certainly smaller than $BDE_{BX}/4$ [see eqns. (14) and (15)] that varies from 63 to100 kJ mol^{-1} for the haloaromatic compounds according to Table 2. Rather, they are relatively closer to the 11 kJ mol^{-1} found for the self-exchange ET reaction of delocalized aromatic radical anions where the reorganization mainly stems from the solvent.[71] The solvent reorganization therefore seems to constitute a substantial part of the intrinsic barrier for the cleavage reactions of $BX^{\bullet-}$ [see eqn. (13)] as found for the radical anions of α-substituted acetophenones, where its contribution was estimated to be as large as 38–67 kJ mol^{-1}.[43] It may seem surprising that the required reorganization of the internal molecular coordinates for the cleavage processes of the haloaromatic radical anions, including the endergonic processes, is relatively modest but this indicates that there must be a substantial weakening of the C–X bond upon injection of an electron in BX.

PM3 calculations

In order to obtain information on the structure of the radical anions semi-empirical PM3 calculations were carried out using the MOPAC program package. In Table 3 we have collected the calculated charges on the halogen atoms as well as the carbon–halogen bond lengths for BX and $BX^{\bullet-}$. For most aryl iodides and bromides, but not chlorides, a substantial amount of the negative charge is positioned on the halogen atoms due to the larger polarizability of iodine and bromine. The same tendency is seen for the lengths of the carbon–halogen bonds in the sense that there is an appreciable elongation of the carbon–iodine and carbon–bromine bonds but not the carbon–chlorine bond on going from the neutral compounds to the radical anions.

This localization of the charge at iodine also explains nicely why the experimentally determined values of E^{o}_{BX} are almost the same for all iodo compounds but the two iodonitrobenzenes. In contrast to this stands the large variation in E^{o}_{BX} for the radical anions of the chloro compounds where the charge is mainly localized at the substituents. The calculations also support the possibility of having different reaction pathways, depending on the substituent. For aryl halides having no or relatively weak electron-withdrawing groups the cleavage reactions are best described as simple decays; the charge is positioned at the halogen atom in the radical anions with a substantial weakening of the carbon–halogen bond as a result. Experimentally, this mechanistic pathway is seen for the exergonic reactions where there is almost no halogen effect on the cleavage rate constants. For the nitro- and carbonyl-substituted aryl halides, on the other hand, the charge density on the halogen atoms in the radical anions is smaller and the carbon–halogen bond is less affected by the presence of the odd electron.§ In these cases the cleavage process can be described as an intra-molecular ET from the substituent on the aryl ring to the σ* orbital of the carbon–halogen bond. Although the mixing of the π* and σ* states is symmetry-forbidden it may proceed through a non-planar geometry with a halogen atom situated out of the plane of the aromatic ring.[72–75] Experimentally, this mechanistic pathway is seen for the more endergonic reactions where the halogen effect on the cleavage rate constants is larger.

§ Presumably the calculations even underestimate the extent of charge localization at these substituents, since they do not take into account solvent effects, *i.e.* the favourable solvation of negatively charged substituents.

Table 3 Semi-empirical PM3 calculations on the substrates, BX, and their radical anions, $BX^{\bullet -}$

BX	Charge ($BX^{\bullet -}$)[a]	Charge (BX)[b]	$r_{BX^{\bullet -}}$[c]	r_{BX}[d]	Δr[e]
Chlorobenzene	−0.2634	0.0628	1.787	1.686	0.101
Bromobenzene	−0.6703	−0.0049	2.195	1.868	0.327
Iodobenzene	−0.5785	0.0175	2.074	1.970	0.104
4-Chlorobenzonitrile	−0.0595	0.0842	1.696	1.682	0.014
4-Bromobenzonitrile	−0.5470	0.0165	2.051	1.866	0.185
4-Iodobenzonitrile	−0.5435	0.0470	2.060	1.968	0.092
Ethyl 4-chlorobenzoate	−0.0574	0.0771	1.696	1.683	0.013
Ethyl 4-bromobenzoate	−0.5125	0.0081	2.028	1.867	0.161
Ethyl 4-iodobenzoate	−0.5474	0.0376	2.061	1.968	0.093
2-Chlorobenzaldehyde	−0.0680	0.0736	1.710	1.689	0.021
2-Chloroacetophenone	−0.0709	0.1020	1.713	1.681	0.032
2-Bromoacetophenone	−0.6683	0.0419	2.232	1.866	0.366
3-Chloroacetophenone	−0.0792	0.0708	1.714	1.687	0.027
3-Bromoacetophenone	−0.6419	0.0059	2.151	1.868	0.283
3-Iodoacetophenone	−0.5578	0.0316	2.067	1.970	0.097
4-Chloroacetophenone	−0.0584	0.0767	1.696	1.683	0.013
4-Bromoacetophenone	−0.5530	0.0076	2.056	1.867	0.189
4-Iodoacetophenone	−0.5512	0.0351	2.063	1.968	0.095
2-Chlorobenzophenone	−0.0087	0.0791	1.697	1.687	0.010
3-Bromobenzophenone	−0.1606	0.0065	1.894	1.867	0.027
4-Chlorobenzophenone	−0.0491	0.0740	1.696	1.684	0.012
4-Bromobenzophenone	−0.1411	0.0049	1.881	1.867	0.014
4-Iodobenzophenone	−0.5474	0.0313	2.061	1.969	0.092
4,4′-Dichlorobenzophenone	−0.0434	0.0759	1.695	1.683	0.012
3-Iodonitrobenzene	−0.5213	0.0699	2.056	1.966	0.090
4-Chloronitrobenzene	−0.0403	0.1013	1.693	1.678	0.015
4-Bromonitrobenzene	−0.1316	0.0306	1.879	1.865	0.014
4-Iodonitrobenzene	−0.4995	0.0676	2.052	1.966	0.086
3-Bromo-4-methylnitrobenzene	−0.6045	0.0343	2.116	1.865	0.251
4-Bromo-3-methylnitrobenzene	−0.1256	0.0305	1.878	1.864	0.014
4-Bromo-3,5-dimethylnitrobenzene	−0.3242	0.0308	1.950	1.864	0.086
1-Bromofluorenone	−0.1036	0.0381	1.888	1.865	0.023
3-Bromofluorenone	−0.1413	0.0050	1.889	1.869	0.020
1-Chloronaphthalene	−0.0535	0.0671	1.702	1.688	0.014
1-Bromonaphthalene	−0.6581	−0.0029	2.190	1.873	0.317
1-Iodonaphthalene	−0.5739	0.0221	2.094	1.974	0.120
2-Chloronaphthalene	−0.0760	0.0636	1.710	1.687	0.023
2-Bromonaphthalene	−0.6505	−0.0049	2.159	1.869	0.290
1-Chloroanthracene	−0.0327	0.0665	1.704	1.689	0.015
2-Chloroanthracene	−0.0494	0.0645	1.705	1.686	0.019
9-Chloroanthracene	−0.0300	0.0745	1.701	1.690	0.011
9-Bromoanthracene	−0.6610	0.0022	2.223	1.875	0.348
9,10-Dichloroanthracene	−0.0220	0.0806	1.700	1.689	0.011
2-Chloropyridine	−0.0902	0.0969	1.720	1.690	0.030
2-Bromopyridine	−0.6176	0.0222	2.139	1.877	0.262
2-Iodopyridine	−0.5279	0.0508	2.071	1.977	0.094
3-Chloropyridine	−0.0803	0.0897	1.700	1.679	0.021
3-Bromopyridine	−0.6264	0.0266	2.135	1.862	0.273
2-Chloroquinoline	−0.0689	0.0890	1.724	1.696	0.028
4-Chloroquinoline	−0.0408	0.0867	1.694	1.682	0.012

[a] Charge on the halogen atom in the radical anion. [b] Charge on the halogen atom in the neutral compound. [c] In Å, the carbon–halogen bond length for the radical anion. [d] In Å, the carbon–halogen bond length for the neutral compound. [e] In Å, the difference in carbon–halogen bond lengths, *i.e.* $\Delta r = r_{BX^{\bullet -}} - r_{BX}$.

According to the Savéant model the expressions for the intrinsic barrier shown in eqns. (14) and (15) depend on whether the electron is localized at the B (*i.e.* for the most endergonic cleavage reactions) or the X part (*i.e.* for the most exergonic reactions) of the molecule. Although the potential terms are not known exactly in the two expressions it would be expected that the endergonic reactions, where there is almost no weakening of the carbon–halogen bond prior to the cleavage process, should have a larger intrinsic barrier than the exergonic processes. On these grounds it may seem peculiar that the intrinsic barrier extracted from the parabolic fit is relatively small for all the cleavage reactions. A possible explanation is that the endergonic reactions, as suggested by recent theoretical investigations,[74,75] proceed by a two-step mechanism, in which the rate-controlling reaction is an ET from the substituent to the carbon–halogen bond to produce a σ* radical anion. This intermediate then dissociates rapidly into the aryl radical and the halide in the second step. Note that the driving force for such a π*–σ* orbital isomerism would differ from the calculated values of $-\Delta G^{\circ}_{BX^{\bullet -}}$ listed in Table 2 which obviously would influence the activation–driving force relationship depicted in Fig. 7. Nevertheless, this does not change the fact that a rough empirical correlation exists between log k_c and $\Delta G^{\circ}_{BX^{\bullet -}}$ for haloaromatic radical anions independent of X.

Conclusions

The kinetic method presented for the determination of large cleavage rate constants, k_c, of radical anions is based on a relatively simple approach and instrumentation. It may be considered as a useful alternative or supplement to direct techniques when their use is prohibited by chemical or technical limitations. We also expect that the approach should be applicable in the study of radical cations. The method requires the presence of a competition between the cleavage reaction of the radical anion under study and a reverse electron transfer

between the radical anion and a suitable electron acceptor. The rate constant for the latter reaction should be known. The method can be considered as an extension of the redox catalysis approach developed by Savéant and co-workers but it possesses some distinct advantages in terms of greater tolerance toward mechanistic changes as well as the possibility of investigating faster cleavage reactions, even when the reverse electron transfer is associated with a large intrinsic barrier. The applicability of the method has been shown by characterizing cleavage reactions of haloaromatic radical anions having rate constants k_c in the range from 10^7 to larger than 2×10^{10} s^{-1}. All haloaromatic radical anions, including the one of iodobenzene, were found to exist when generated in the homogeneous reduction process. In general, k_c is found to increase in the halogen order Cl < Br < I, the exceptions being for the series of 2- and 3-halopyridine radical anions, where no clear trend was observable.

A rough quadratic correlation exists between log k_c and $\Delta G^{\circ}_{BX^{\bullet-}}$, even if there seem to be two limiting mechanistic pathways present for the radical anions studied. For aryl halides having no or relatively weak electron-withdrawing groups the most exergonic cleavage reactions are best described as simple decays, where a significant amount of the electron density in the radical anion is placed on the halogen atom. For the nitro- and carbonyl-substituted aryl halides, on the other hand, the electron density is mainly located on the substituent and there is essentially no weakening of the carbon–halogen bond in the radical anion prior to the endergonic cleavage reaction. In spite of these mechanistic differences a relatively low overall intrinsic barrier of 27–39 kJ mol^{-1} is found for all the cleavage reactions. This points towards the possibility of having a stepwise mechanism for the endergonic processes, in which a σ* radical anion is formed as intermediate prior to the formation of the dissociated products, the aryl radical and the halide. Small intrinsic barriers have also been reported in the literature for α-aryloxyacetophenone radical anions and bibenzylic radical anions and cations suggesting that the influence of the specific molecular structure on the intrinsic barriers for the cleavage reaction of many chemical systems is relatively small.

Experimental

Materials

Most of the aromatic halides (chloro-, bromo- and iodobenzene, 1-chloro-, 1-bromo-, 2-bromo- and 1-iodonaphthalene, ethyl 4-bromobenzoate, 2-bromo- and 4-iodoacetophenone, 4-chloro- and 4-bromobenzonitrile and 2-chloro-, 3-chloro-, 2-bromo- and 3-bromopyridine) and mediators (anthracene, 1,4-dicyanobenzene, fluoranthene, quinoxaline, phenazine, benzanthrone, fluoren-9-one, 2-naphthonitrile, *m*-toluonitrile, (*E*)-azobenzene and (*E*)-4-methoxycarbonylazobenzene) were commercially available or used previously.[48] (*E*)-2,4-Dimethoxyazobenzene was prepared as described in ref. 76. 4-Iodobenzonitrile was synthesised by diazotisation of 4-aminobenzonitrile followed by substitution of the diazonium group by iodide.[77] The same method was employed in the synthesis of 3-iodoacetophenone from 3-aminoacetophenone. 2-Iodopyridine was prepared by refluxing 2-bromopyridine with HI (57%) for six hours followed by extraction with diethyl ether.[78] Ethyl 4-chlorobenzoate and ethyl 4-iodobenzoate were synthesised by reacting ethanol with the corresponding acyl chlorides, prepared by standard procedures from 4-chloro- and 4-iodobenzoic acid, respectively. 4-Iodobenzophenone was prepared by a Friedel–Crafts acylation of iodobenzene by benzoyl chloride.[79] All chemicals were purified by distillation or recrystallization; ^{1}H-NMR and ^{13}C-NMR spectra were recorded to check the level of purity. The solvent *N*,*N*-dimethylformamide (DMF) was obtained from Aczo and the supporting electrolyte tetrabutylammonium tetrafluoroborate (Bu_4NBF_4) was prepared using standard procedures. The solution consisting of 0.1 M Bu_4NBF_4 in DMF was dried prior to use by passing it through a column containing activated alumina (ICN Alumina N, Super 1, ICN Biomedicals). The solution was degassed with argon (99.99%).

Apparatus

A detailed description of the stopped-flow UV,[80] the UV dip probe[80] and the rotating disc electrode apparatus[81–83] is given in the references listed.

Procedures

Stopped-flow UV technique. A degassed 0.1 M $TBABF_4$–DMF solution containing the aromatic compound, A, in a concentration of about 1 mM was passed from a syringe through the inlet hole of the flow cell to the chamber containing the working electrode and the reference electrode. As the aromatic compound passed the working electrode an efficient preparative reduction was carried out using a three-electrode set-up at a constant potential corresponding to the standard potential of A. The solution was led through the outlet to the mixing chamber of the UV spectrometer, where it was mixed with an equally large volume of a degassed solution from another syringe containing the substrate BX and additional A. The initial concentration of the radical anion $A^{\bullet-}$ was normally 0.1 mM as deduced from the UV spectrum¶ although it should be noted that the exact concentration of $A^{\bullet-}$ has no importance for the measurements as long as the reaction kinetics is constrained to pseudo-first-order conditions. The concentrations of BX and A were in the range from 5 to 100 mM and 1 to 600 mM, respectively. The decay of the radical anion due to the reaction with the substrate was followed in an appropriate wavelength range encompassing the maximal absorption peak and the characteristic parameter denoted γ could be obtained in the kinetic treatment [see eqns. (7) and (8)]. The measurements were performed at least three times for each concentration of A. Experiments without the substrate being present were always conducted in order to determine the stability of the radical anion and ensure that its "natural decay" had no influence on the actual decay recorded. The γ values accessible by this method are in the range $10^{-2} - 500$ M^{-1} s^{-1}.

UV dip probe technique. 40 mL 0.1 M $TBABF_4$–DMF solution containing the aromatic compound, A, in the cathodic compartment of an H-cell were degassed with argon. While the solution was stirred with a magnetic bar, preparative reduction of A was commenced at its standard potential at a platinum net with a carbon rod in the anodic chamber serving as counter electrode. During this reduction process UV spectra in the wavelength region 300–750 nm were recorded by means of the dip probe positioned in the cathodic compartment. The potentiostat was disconnected as the maximal absorbance of $A^{\bullet-}$ approached one for a light path length of 10 mm. For most $A^{\bullet-}$ this corresponds to a concentration of 0.1–0.5 mM. In order to check the stability of $A^{\bullet-}$ its decay was recorded as a function of time at an appropriate wavelength, in most cases corresponding to the maximal absorption peak. If the half life was found to be high (>500 s), addition of the substrate in large excess followed. The pseudo-first-order decay of $A^{\bullet-}$ was recorded and kinetic treatment allowed the determination of γ [see eqns. (7) and (8)]. The experiments could be repeated several times with the same solution and set-up by carrying out first a preparative reduction of a certain amount of A to $A^{\bullet-}$ as fast as possible and subsequently recording its decay. The same cell could even be used to obtain γ for other values of [A] by adding the aromatic compound in the amount required to the cell and then repeating the procedure just described. The concentrations of BX and A used were 5–100 mM and 1–600 mM, respectively.

¶ Relevant extinction coefficients are given in ref. 80.

The γ values accessible by this method are in the range $10^{-3} - 10\ M^{-1}\ s^{-1}$.

Rotating disc electrode technique. The procedure was the same as described above just having the dip probe replaced by a rotating disc electrode. According to the Levich equation[84] the plateau oxidation current of $A^{\bullet -}$ at the rotating disk electrode is proportional to the bulk concentration, thus allowing the decay of $A^{\bullet -}$ to be followed by electrochemical means. The γ values accessible by this method are in the range $10^{-3} - 10\ M^{-1}\ s^{-1}$.

Comments

The applicability of the three techniques is more or less alike. The stopped-flow method has a larger time window and can be used advantageously in the study of faster reactions. Note that if the same solution is used to determine γ for several values of [A] in the UV dip probe and rotating disc electrode techniques, any influence on the reaction kinetics from long term product build-up should be checked by repeating one or more of the experiments on fresh solutions. The use of UV–VIS detection may in some cases be associated with difficulties if products with strong absorption bands are formed and in such instances the electrochemical detection mode is to be preferred.

PM3 calculations

All calculations were performed with the MOPAC program package. The unrestricted Hartree–Fock method was used for the radical anions, $BX^{\bullet -}$, and radicals, $B^{\bullet}$, and the restricted Hartree–Fock method was used for the neutral compounds, BX. The bond dissociation energies were determined relative to the experimentally available bond dissociation energies of chloro-, bromo-, and iodobenzene[85] using calculated values of the enthalpies of formation, ΔH_f. If $\Delta\Delta H$ is defined as $\Delta H_{f,B^{\bullet}} - \Delta H_{f,BX}$, the relative bond dissociation energy is given by: $\Delta BDE = \Delta\Delta H(\text{substrate}) - \Delta\Delta H(\text{halobenzene})$. The bond dissociation energy for the substrate is subsequently obtained as $BDE(\text{substrate}) = BDE(\text{halobenzene}) + \Delta BDE$.

References

1 J. G. Lawless and M. D. Hawley, *J. Electroanal. Chem.*, 1969, **21**, 365.
2 L. Nadjo and J.-M. Savéant, *J. Electroanal. Chem.*, 1971, **30**, 41.
3 B. Aalstad and V. D. Parker, *Acta Chem. Scand.*, 1982, **B36**, 47.
4 C. P. Andrieux, A. Le Gorande and J.-M. Savéant, *J. Am. Chem. Soc.*, 1992, **114**, 6892.
5 D. O. Wipf and R. M. Wightman, *J. Phys. Chem.*, 1989, **93**, 4286.
6 R. K. Norris, S. D. Barker and P. Neta, *J. Am. Chem. Soc.*, 1984, **106**, 3140.
7 P. Neta and D. Behar, *J. Am. Chem. Soc.*, 1980, **102**, 4798.
8 P. Neta and D. Behar, *J. Am. Chem. Soc.*, 1981, **103**, 103.
9 D. Behar and P. Neta, *J. Am. Chem. Soc.*, 1981, **103**, 2280.
10 K. Sehested and J. Holcman, *J. Phys. Chem.*, 1978, **82**, 651.
11 N. Mathivanan, L. J. Johnston and D. D. M. Wayner, *J. Phys. Chem.*, 1995, **99**, 8190.
12 G. V. Buxton and Q. G. Mulazzani, in *Electron Transfer in Chemistry*, ed. V. Balzani, Wiley, Weinheim, 2001, Vol. 1, Part 2, ch. 3.
13 K. Henbest and M. A. J. Rodgers, in *Electron Transfer in Chemistry*, ed. V. Balzani, Wiley, Weinheim, 2001, Vol. 1, Part 2, ch. 4.
14 V. V. Konovalov, A. M. Raitsimring and Y. D. Tsvetkov, *Chem. Phys. Lett.*, 1989, **157**, 257.
15 V. V. Konovalov, I. I. Bilkis, B. A. Selivanov, V. D. Shteingarts and Y. D. Tsvetkov, *J. Chem. Soc., Perkin Trans. 2*, 1993, 1707.
16 R. S. Nicholson and I. Shain, *Anal. Chem.*, 1964, **36**, 706.
17 C. P. Andrieux, J. M. Dumas-Bouchiat and J.-M. Savéant, *J. Electroanal. Chem.*, 1978, **87**, 39.
18 C. P. Andrieux, J. M. Dumas-Bouchiat and J.-M. Savéant, *J. Electroanal. Chem.*, 1978, **88**, 43.
19 C. P. Andrieux, J. M. Dumas-Bouchiat and J.-M. Savéant, *J. Electroanal. Chem.*, 1978, **87**, 55.
20 C. P. Andrieux, C. Blocman, J.-M. Dumas-Bouchiat and J.-M. Savéant, *J. Am. Chem. Soc.*, 1979, **101**, 3431.
21 C. P. Andrieux, C. Blocman, J. M. Dumas-Bouchiat, F. M'Halla and J.-M. Savéant, *J. Am. Chem. Soc.*, 1980, **102**, 3806.
22 C. P. Andrieux and J.-M. Savéant, *J. Electroanal. Chem.*, 1986, **205**, 43.
23 T. B. Christensen and K. Daasbjerg, *Acta Chem. Scand.*, 1997, **51**, 307.
24 C. P. Andrieux, J.-M. Savéant and D. Zann, *Nouv. J. Chim.*, 1984, **8**, 107.
25 J.-M. Savéant, *Acc. Chem. Res.*, 1993, **26**, 455.
26 C. P. Andrieux, M. Robert, F. D. Saeva and J.-M. Savéant, *J. Am. Chem. Soc.*, 1994, **116**, 7864.
27 W. Adcock, C. P. Andrieux, C. I. Clark, A. Neudeck, J.-M. Savéant and C. Tardy, *J. Am. Chem. Soc.*, 1995, **117**, 8285.
28 M. Meot-Ner, P. Neta, R. K. Norris and K. Wilson, *J. Phys. Chem.*, 1986, **90**, 168.
29 C. P. Andrieux, E. Differding, M. Robert and J.-M. Savéant, *J. Am. Chem. Soc.*, 1993, **115**, 6592.
30 J. Masnovi, *J. Am. Chem. Soc.*, 1989, **111**, 9081.
31 H. Jensen and K. Daasbjerg, *Acta Chem. Scand.*, 1998, **52**, 1151.
32 N. Kimura and S. Takamuku, *Bull. Chem. Soc. Jpn.*, 1992, **65**, 1668.
33 N. Kimura and S. Takamuku, *J. Am. Chem. Soc.*, 1995, **117**, 8023.
34 D. O. Wipf and R. M. Wightman, *Anal. Chem.*, 1990, **62**, 98.
35 J. S. Jaworski, P. Leszczyński and J. Tykarski, *J. Chem. Res. (S)*, 1995, 510.
36 C. P. Andrieux, M. Robert and J.-M. Savéant, *J. Am. Chem. Soc.*, 1995, **117**, 9340.
37 K. Daasbjerg, H. Jensen, R. Benassi, F. Taddei, S. Antonello, A. Gennaro and F. Maran, *J. Am. Chem. Soc.*, 1999, **121**, 1750.
38 S. Jakobsen, H. Jensen, S. U. Pedersen and K. Daasbjerg, *J. Phys. Chem. A*, 1999, **103**, 4141.
39 S. Antonello and F. Maran, *J. Am. Chem. Soc.*, 1999, **121**, 9668.
40 J. M. Tanko and J. P. Phillips, *J. Am. Chem. Soc.*, 1999, **121**, 6078.
41 Z.-R. Zheng, D. H. Evans, E. S. Chan-Shing and J. Lessard, *J. Am. Chem. Soc.*, 1999, **121**, 9429.
42 P. Maslak, T. M. Vallombroso, W. H. Chapman Jr. and J. N. Narvaez, *Angew. Chem., Int. Ed. Engl.*, 1994, **33**, 73.
43 C. P. Andrieux, J.-M. Savéant, A. Tallec, R. Tardivel and C. Tardy, *J. Am. Chem. Soc.*, 1996, **118**, 9788.
44 C. P. Andrieux, J.-M. Savéant, A. Tallec, R. Tardivel and C. Tardy, *J. Am. Chem. Soc.*, 1997, **119**, 2420.
45 M. L. Andersen, N. Mathivanan and D. D. M. Wayner, *J. Am. Chem. Soc.*, 1996, **118**, 4871.
46 M. L. Andersen, W. Long and D. D. M. Wayner, *J. Am. Chem. Soc.*, 1997, **119**, 6590.
47 S. Antonello and F. Maran, *J. Am. Chem. Soc.*, 1998, **120**, 5713.
48 D. Occhialini, J. S. Kristensen, K. Daasbjerg and H. Lund, *Acta Chem. Scand.*, 1992, **46**, 474.
49 N. T. Kjær and H. Lund, *Acta Chem. Scand.*, 1995, **49**, 848.
50 G. Grampp and W. Jaenicke, *Ber. Bunsen-Ges. Phys. Chem.*, 1991, **95**, 904.
51 L. Pause, M. Robert and J.-M. Savéant, *J. Am. Chem. Soc.*, 1999, **121**, 7158.
52 J. Keizer, *J. Phys. Chem.*, 1982, **86**, 5052.
53 J. Keizer, *Chem. Rev.*, 1987, **87**, 167.
54 J. Grimshaw and N. Thompson, *J. Electroanal. Chem.*, 1986, **205**, 35.
55 F. M'Halla, J. Pinson and J.-M. Savéant, *J. Am. Chem. Soc.*, 1980, **102**, 4120.
56 C. Amatore, M. A. Oturan, J. Pinson, J.-M. Savéant and A. Thiébault, *J. Am. Chem. Soc.*, 1985, **107**, 3451.
57 D. D. Tanner, J. J. Chen, L. Chen and C. Luelo, *J. Am. Chem. Soc.*, 1991, **113**, 8074.
58 C. P. Andrieux, P. Hapiot and J.-M. Savéant, *J. Phys. Chem.*, 1988, **92**, 5987.
59 V. D. Parker, *Acta Chem. Scand.*, 1981, **B35**, 655.
60 W. C. Danen, T. T. Kensler, J. G. Lawless, M. F. Marcus and M. D. Hawley, *J. Phys. Chem.*, 1969, **73**, 4389.
61 J. S. Jaworski, P. Leszczyński and S. Filipek, *J. Electroanal. Chem.*, 1997, **440**, 163.
62 W. B. Davis, W. A. Svec, M. A. Ratner and M. R. Wasielewski, *Nature*, 1998, **396**, 60.
63 K. Daasbjerg, *J. Chem. Soc., Perkin Trans. 2*, 1994, 1275.
64 N. Kornblum, *Angew. Chem.*, 1975, **87**, 797.
65 J. F. Bunnett, *Acc. Chem. Res.*, 1978, **11**, 413.
66 J.-M. Savéant, *Acc. Chem. Res.*, 1980, **13**, 323.
67 P. Wardman, *J. Phys. Chem. Ref. Data*, 1989, **18**, 1637.
68 Y. Marcus, M. J. Kamlet and R. W. Taft, *J. Phys. Chem.*, 1988, **92**, 3613.
69 A. Anne, S. Fraoua, J. Moiroux and J.-M. Savéant, *J. Am. Chem. Soc.*, 1996, **118**, 3938.
70 J.-M. Savéant, *J. Phys. Chem.*, 1994, **98**, 3716.
71 H. Larsen, S. U. Pedersen, J. A. Pedersen and H. Lund, *J. Electroanal. Chem.*, 1992, **331**, 971.

72 K. E. Miller and J. J. Kozak, *J. Phys. Chem.*, 1985, **89**, 401.
73 L. N. Shchegoleva, I. I. Bilkis and P. V. Schastnev, *Chem. Phys. Lett.*, 1984, **104**, 348.
74 A. B. Pierini and J. S. Duca Jr., *J. Chem. Soc., Perkin Trans. 2*, 1995, 1821.
75 A. B. Pierini, J. S. Duca Jr. and D. M. A. Vera, *J. Chem. Soc., Perkin Trans. 2*, 1999, 1003.
76 K. Kokkinos and R. Wizinger, *Helv. Chim. Acta*, 1971, **54**, 330.
77 S. J. Brown, J. H. Clark and D. J. Macquarrie, *J. Chem. Soc., Dalton Trans.*, 1988, 277.
78 W. Barker, R. F. Curtis and M. G. Edwards, *J. Chem. Soc.*, 1951, 83.
79 E. Bergmann, H. Hoffmann and H. Meyer, *J. Prakt. Chem.*, 1932, **135**, 245.
80 S. U. Pedersen, T. B. Christensen, T. Thomasen and K. Daasbjerg, *J. Electroanal. Chem.*, 1998, **454**, 123.
81 S. U. Pedersen and K. Daasbjerg, *Acta Chem. Scand.*, 1989, **43**, 301.
82 K. Daasbjerg, S. U. Pedersen and H. Lund, *Acta Chem. Scand.*, 1989, **43**, 876.
83 K. Daasbjerg, S. U. Pedersen and H. Lund, *Acta Chem. Scand.*, 1991, **45**, 424.
84 A. J. Bard and L. R. Falkner, *Electrochemical Methods: Fundamentals and Applications*, 1st edn., Wiley, New York, 1980.
85 *Handbook of Chemistry and Physics*, ed. D. R. Lide, 72nd edn., CRC Press, Boca Raton, 1991.